Journal of Molecular Structure 1041 (2013) 23–28

Contents lists available at SciVerse ScienceDirect

Journal of Molecular Structure

journal homepage: www.elsevier.com/locate/molstruc

Crystal structure refinement and vibrational analysis of $Y[Co(CN)_6]\cdot 4H_2O$ and its thermal decomposition products

Diego M. Gil [a], Raúl E. Carbonio [b,1], M. Inés Gómez [a,*]

[a] Instituto de Química Inorgánica, Facultad de Bioquímica, Química y Farmacia, Universidad Nacional de Tucumán, Ayacucho 471, 4000 San Miguel de Tucumán, Argentina
[b] INFIQC (CONICET), Departamento de Fisicoquímica, Facultad de Ciencias Químicas, Universidad Nacional de Córdoba, Ciudad Universitaria, X5000HUA Córdoba, Argentina

HIGHLIGHTS

- The cyano complex $Y[Co(CN)_6]\cdot 4H_2O$ was synthesized and its crystal structure was refined by means the Rietveld analysis.
- The complex crystallizes in the orthorhombic crystal system, space group *Cmcm*.
- The vibrational behavior of the complex $Y[Co(CN)_6]\cdot 4H_2O$ was analyzed using IR and Raman spectroscopy.
- The thermal treatments of $Y[Co(CN)_6]\cdot 4H_2O$ in air produce the mixed oxide $Y_{1-x}CoO_3$.
- We refine the crystal structure of $YCoO_3$ obtained at 950 °C and we found that it was slightly deficient in Y^{3+}.

ARTICLE INFO

Article history:
Received 12 December 2012
Received in revised form 4 March 2013
Accepted 5 March 2013
Available online 13 March 2013

Keywords:
Crystal structure refinement
Thermal decomposition
$YCoO_3$
Raman spectroscopy

ABSTRACT

Studies on $Y[Co(CN)_6]\cdot 4H_2O$ by means of thermal analysis, IR and Raman spectroscopy and X-ray powder diffraction were carried out. The complex $Y[Co(CN)_6]\cdot 4H_2O$ crystallizes in the orthorhombic crystal system, space group *Cmcm*. Y^{3+} ion is eight-coordinated forming bicapped distorted trigonal prism YN_6O_2 and Co^{3+} ion is octahedrally coordinated to six CN groups. The IR spectrum shows well-resolved bands in the CN stretching region due to the presence of ^{13}C and ^{15}N in relative natural abundance. The Raman spectrum of the complex shows two distinct set of bands of the CN stretching vibration: one is a singlet and the other is split due to the low symmetry of the Y^{3+} ion compared to the pentahydrate complex. The thermal decomposition was studied in order to investigate the formation of $YCoO_3$. The crystal structure of $YCoO_3$ was refined by means of Rietveld analysis using PXRD data. We found that it was slightly deficient in Y^{3+}, which is in agreement with the small amount of Y_2O_3 found as impurity in the sample. The formula of the mixed oxide obtained by this method of synthesis is $Y_{0.961}CoO_3$.

1. Introduction

The structure and properties of rare-earth hexacyanometallates (III) hydrates, $Ln[M(CN)_6]\cdot nH_2O$ (Ln = lanthanide; M = transition metal; $n = 4$ or 5) have been widely investigated for a long time, but systematic studies on a series of hexacyanometallate complexes have not yet been carried out. Generally, in hexacyanometallates the metal centers are usually found bridged by CN groups where the C and N ends remain linked to only one metal. The metal linked at the C end is always with octahedral coordination to form the anionic hexacyanometallate octahedral block, $[M^n(CN)_6]^{6-n}$. The 3D framework is formed when neighboring blocks are linked at their N end through a second metal, in this case a rare-earth metal. The CN ligand has the ability to serve as bridge group between neighboring metal centers, removing electron density from the metal linked at the C end, through a π back-bonding interaction, to increase the charge density on the end N that is the coordination site for the other metal. This process leads to the overlapping between the electron clouds of neighboring metal centers and to their spin coupling and, thereby, a magnetic ordering is established. This supports the role of hexacyanometalltes as prototype of molecular magnets [1–4].

Hulliger et al. have reported in their investigations that $Ln[Co(CN)_6]\cdot nH_2O$ crystallize in the hexagonal or orthorhombic crystal system depending on the number of water molecules and the size of lanthanide ions. Large Ln (III) ions in the series of hexacyanocobaltates salts crystallize as pentahydrates in the hexagonal crystal system and small Ln (III) ions produce tetrahydrated complexes with an orthorhombic crystal structure [5]. The limit between both hydrates is in the Nd^{3+} compound where both, the tetra- and pentahydrates are stable [6].

The heteronuclear complexes $Ln[M(CN)_6]\cdot nH_2O$ are precursors for the synthesis of perovskite-type oxides which have a variety

* Corresponding author. Tel.: +54 381 4247752x7069.
E-mail address: mgomez@fbqf.unt.edu.ar (M. Inés Gómez).
[1] Member of the Research Career of CONICET.

0022-2860/$ - see front matter © 2013 Elsevier B.V. All rights reserved.
http://dx.doi.org/10.1016/j.molstruc.2013.03.008

of applications such as chemical sensors, catalysts and multiferroic materials [7–11]. Traditionally, the ceramic method has been employed to synthesize mixed oxides. However, this method usually needs very high temperatures to reach chemical homogeneity, producing very low surface areas and oxygen deficient materials. The thermal decomposition of heteronuclear complexes was proposed by Gallagher in 1968 to prepare $LaFeO_3$ and $LaCoO_3$ from hexacyanometallates as precursors [12]. The oxides obtained by this method were formed at shorter annealing times and lower temperatures than ceramic methods. The use of a precursor containing the appropriate A/B ratio enforces the formation of ABO_3 perovskites with the precise stoichiometry, thus controlling and preventing any elements segregation generally observed in conventional methods and allowing the synthesis of the desired mixed oxide at very low temperatures [12–19]. The homogeneous mixed oxides so obtained have relatively high surface areas and consequently can be used as catalyst in different chemical reactions [20].

In the present article we report the crystal structure refinement and vibrational characterization of $Y[Co(CN)_6]\cdot 4H_2O$ and its thermal decomposition products. The crystal structure refinement of the complex was performed by Rietveld Analysis using conventional powder X-ray diffraction (PXRD) data. These measurements were complemented by thermogravimetric and differential thermal analysis and IR and Raman spectroscopy. The thermal decomposition products were characterized by IR and Raman spectroscopy and the crystal structure refinement of obtained $Y_{1-x}CoO_3$ was performed by means of Rietveld analysis of PXRD data.

2. Experimental

The polycrystalline sample of $Y[Co(CN)_6]\cdot 4H_2O$ was prepared by the co-precipitation method, mixing aqueous solutions of equimolar amounts of $K_3[Co(CN)_6]$ and $Y(NO_3)_3\cdot 6H_2O$ under continuous stirring at 60 °C for 2 h. $Y(NO_3)_3\cdot 6H_2O$ was prepared from the evaporation of a solution of concentrated HNO_3 and Y_2O_3. The white resulting precipitate was filtered, washed many times with distilled water and ethanol, and finally stored in a dry box with silica gel.

Thermogravimetry (TG) and differential thermal analysis (DTA) curves were performed in a Shimadzu TGA/DTA-50 in the temperature range from 20 to 800 °C at a heating rate of 5°/min under flowing air.

Infrared spectra (in the region of 4000–400 cm^{-1}) were recorded at room temperature (RT) on a FTIR Perkin Elmer 1600 spectrophotometer in the transmission mode using KBr pellets.

The Raman spectra were recorded on a Thermoscientific DXR Raman Microscope. The exciting line was 532 nm being provided by a DXR 532 nm laser.

PXRD patterns were obtained at RT in a PANalytical X'Pert Pro diffractometer with CuKα radiation $\lambda = 1.5418$ Å, between 5° and 120° in 2θ, in steps of 0.02° and step time of 10 s. The crystal structure refinement of $Y[Co(CN)_6]\cdot 4H_2O$ and $YCoO_3$ were performed by means of the Rietveld method [21] using the FULLPROF program [22]. For Yttrium hexacyanocobaltate (III) tetrahydrate, the refinement was made in the space group *Cmcm* using as initial model the structure of $Er[Fe(CN)_6]\cdot 4H_2O$ [23]. A pseudo-Voigt function convoluted with an axial divergence asymmetry function [24] was chosen to generate the peak shapes. The following parameters were refined: zero-point, scale factor, pseudo-Voigt parameters of the peak shape full-width at half-maximum, atomic positions and cell parameters.

3. Results and discussion

3.1. Crystal structure refinement

The powder XRD of $Y[Co(CN)_6]\cdot 4H_2O$ refined at RT is shown in Fig. 1. No impurities were observed in the pattern. Final cell parameters, atomic positions and discrepancy parameters are shown in Table 1.

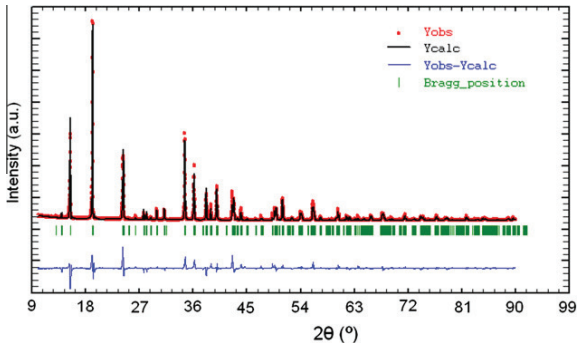

Fig. 1. Rietveld refinement of PXRD patterns for $Y[Co(CN)_6]\cdot 4H_2O$. The dotted line is the observed X-ray diffraction profile and the solid line is the calculated one. The button curve shows the difference of observed and calculated ones and the vertical lines correspond to the allowed Bragg reflections.

Table 1
Crystallographic parameters for $Y[Co(CN)_6].4H_2O$ after Rietveld refinement with PXRD data obtained at RT.

Atom	Wyckoff site	*x*	*y*	*z*
Y	4c	0	0.3254(4)	0.25
Co	4a	0	0	0
C1	16 h	0.310(3)	0.4561(2)	0.0979(1)
C2	8f	0	0.118(3)	0.063(2)
N1	16 h	0.1989(2)	0.4334(1)	0.1332(1)
N2	8f	0	0.2008(2)	0.0752(2)
O1	8 g	0.297(2)	0.2123(1)	0.25
O2	8f	0	0.6597(2)	0.1039(9)

Space group: *Cmcm*; Cell parameters: $a = 7.2947(1)$ Å, $b = 12.6654(2)$ Å, $c = 13.5224(2)$ Å, Vol = 1249.34(3) $Å^3$, $Z = 4$.
Discrepancy factors: $R_{wp} = 20.3$, $R_{exp} = 4.85$, $R_p = 15.5$, $R_{Bragg} = 10.9$.

Fig. 2 shows the coordination environment for Y^{3+} and Co^{3+} ions. The complex $Y[Co(CN)_6]\cdot 4H_2O$ crystallizes in the orthorhombic system, space group *Cmcm* ($a = 7.2947(1)$ Å, $b = 12.6654(2)$ Å, $c = 13.5224(2)$ Å, $V = 1249.34(3)$ $Å^3$, and $Z = 4$). In the crystal structure Y^{3+} ions are 8 – coordinated to four N(1), two N(2) and two O(1) atoms of water molecules forming a bicapped distorted trigonal prism (YN_6O_2). Co^{3+} ions are coordinated to four C(1) and two C(2) forming an irregular octahedral group CoC_6. Both coordination

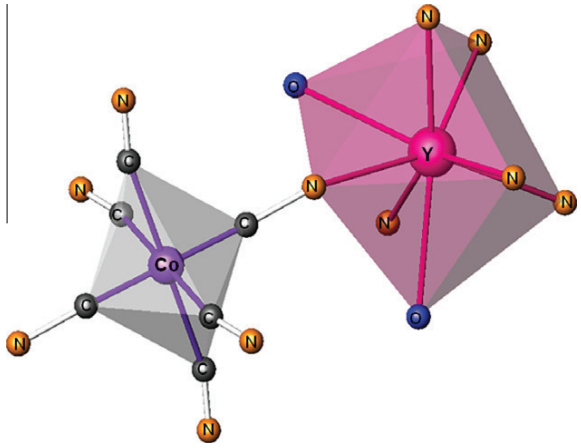

Fig. 2. Coordination environment for Y^{3+} and Co^{3+} ions in $Y[Co(CN)_6]\cdot 4H_2O$.

Table 2
Some selected bond lengths and angles for $Y[Co(CN)_6]\cdot 4H_2O$.

Interatomic distances (Å)		Bond angles (°)	
Y—N		(N1)—(Y)—(N1)	114.9(9)
(Y)—(N1)	2.544(2)	(N2)—(Y)—(N2)	112.5(1)
(Y)—(N2)	2.84(2)	(N1)—(Y)—(N2)	77.4(9)
		(N1)—(Y)—(N2)	144.6(1)
Y—O		(O1)—(Y)—(O1)	113.1(9)
(Y)—(O1)	2.597(2)	(O1)—(Y)—(N1)	79.7(8)
		(O1)—(Y)—(N1)	140.6(1)
Co—C		(O1)—(Y)—(N2)	72.2(8)
(Co)—(C1)	2.00(2)	(C1)—(Co)—(C1)	92.0(1)
(Co)—(C2)	1.72(4)	(C1)—(Co)—(C1)	180.0(2)
C—N		(C1)—(Co)—(C1)	88.0(2)
(C1)—(N1)	1.06(2)	(C1)—(Co)—(C2)	85.0(2)
(C2)—(N2)	1.144(1)	(C1)—(Co)—(C2)	95.0(2)
(O1)···(O2)	2.557(1)	(C2)—(Co)—(C2)	180.0(4)

polyhedra, YN_6O_2 and CoC_6 are bridged through CN groups. The number of crystal water in the unit cell is determined to be 4, being in good agreement with TG-DTA results (see below). In addition, the uncoordinated water molecules are linked to the coordinated water molecules through a weak hydrogen bond. This crystal structure is very similar to $Ln[Co(CN)_6]\cdot 4H_2O$, Ln = Nd [25], Sm [26] and Er [27]. The Y^{3+} ion has a large size (0.900 Å) and shows similarity in chemical and structural behavior with lanthanide (III) ions. Lanthanide ions with a large size such as La, Pr and Nd could form pentahydrate complexes and metals with a minor size such as Sm, Eu, Gd could form tetrahydrate complexes [5,6]. The Y^{3+} ion has the correct size for an 8-fold coordination and only forms stable tetrahydrate hexacyanometallates.

Some selected bond lengths and angles for $Y[Co(CN)_6]\cdot 4H_2O$ are given in Table 2. The CN bond distance does not differ from standard values [3,6,23,25–27]. The Co—C, Y—N and Y—O distances are larger compared with Nd, Sm and Er cobalticyanides [25–27].

3.2. Vibrational analysis

Fig. 3 shows the IR spectrum between 4000 and 400 cm^{-1} for $Y[Co(CN)_6]\cdot 4H_2O$ at room temperature in KBr disks. The inset shows the region between 2220 and 2000 cm^{-1} in more detail. The Raman spectrum for the complex measured at RT is shown in Fig. 4. The analysis of the results confirms the structural data determined by PXRD. The assignment of the experimental bands of the IR and Raman spectra was made in comparison with related

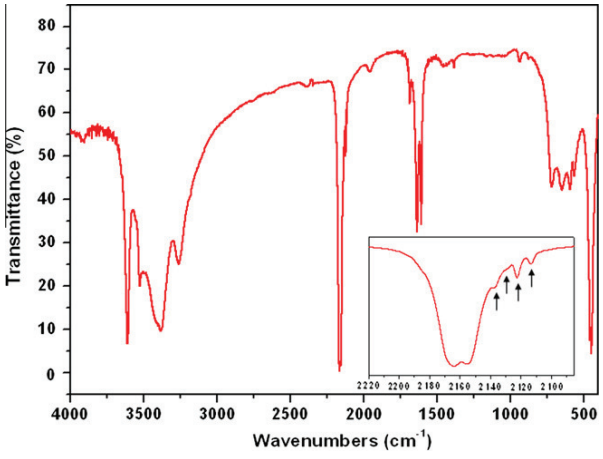

Fig. 3. IR spectrum for $Y[Co(CN)_6]\cdot 4H_2O$ in the 4000–400 cm^{-1}. The inset shows the region between 2200 and 2000 cm^{-1} in more detail.

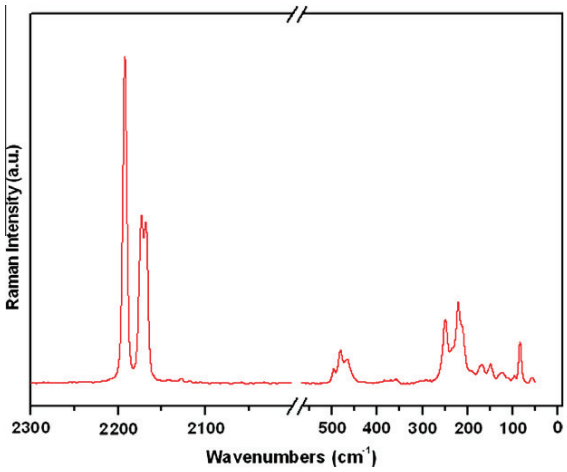

Fig. 4. Raman spectra of $Y[Co(CN)_6]\cdot 4H_2O$.

molecules. The details of the IR and Raman spectra, together with a tentative assignment, are collected in Table 3.

In $Y[Co(CN)_6]\cdot 4H_2O$, the factor group is D_{2h} and the sites symmetries for Y and Co are C_{2v} and C_{2h}, respectively. The Y atom is associated with A_g, B_{2u}, B_{3g}, B_{1u} and B_{3u} modes, and Co atom with A_u, 2 B_{1u} and 2 B_{3u} modes, respectively. The modes of A_u, B_{1u}, B_{2u} and B_{3u} are IR active [36].

3.2.1. C≡N stretching bands

The two strong bands located at 2163 and 2154 cm^{-1} in the IR spectrum are assigned to antisymmetric $^{12}C^{14}N$ stretching bands. The CN stretching in $Y[Co(CN)_6]\cdot 4H_2O$ is at higher wavenumber than in $K_3[Co(CN)_6]$ (2130 cm^{-1}) [28] which reflects the formation of the Y—N≡C—Co bridge. The four weak bands to lower wavenumbers, marked by vertical lines (inset Fig. 3), could be assigned to $^{13}C^{14}N$ and $^{12}C^{15}N$ stretching bands. The Raman spectra (Fig. 4) shows two distinct ν(CN) bands: one was a singlet located at 2192 cm^{-1} and the other was split into two components at 2174 and 2168 cm^{-1}. The splitting observed in these bands is attributed to the low symmetry around the Y atom (8 – coordinated) compared with pentahydrate complexes containing lanthanide ions in which the Ln^{3+} are 9 – coordinated [29]. These bands could be assigned to the symmetric stretching vibration of the Y—N≡C—Co bridges.

3.2.2. M—C≡N and M—C bands

The bands at 590 and 563 cm^{-1} in the IR spectrum are assigned to the CoCN bending mode and the band located at 455 cm^{-1} is assigned to the antisymmetric stretching mode of the C—Co—C vibrations. At lower wavenumbers, the deformation and torsional modes were mainly observed in the solid Raman spectrum. The band observed at 496 cm^{-1} is assigned to the CoCN bending mode and the bands located at 481 and 466 cm^{-1} are assigned to the symmetric stretching mode of C—Co—C vibrations. The band at 85 cm^{-1} could be assigned to a combination of two modes: δ(CoCN) and δ(C—Co—C).

3.2.3. Water bands

The presence of two kinds of crystallographically inequivalent water molecules in the lattice is evidenced by their IR characteristic vibrational modes. The two narrow bands observed at 3610 and 3527 cm^{-1} are assigned to the ν(OH) stretching modes corresponding to water molecules coordinated to Y atoms (see Section 3.1.). The broad bands located at 3380 and 3259 cm^{-1} are

Table 3
Frequencies (cm^{-1}) and observed bands in the Infrared and Raman spectra of $Y[Co(CN)_6]\cdot 4H_2O$.

Infrared	Raman	Approximate description
3610	–	ν(OH) coordinate water
3527	–	ν(OH) coordinate water
3380	–	ν(OH) uncoordinate water
3259	–	ν(OH) uncoordinate water
–	2192	ν_s(CN)
–	2174	ν_s(CN)
–	2168	ν_s(CN)
2163	–	$\nu_a(^{12}C^{14}N)$
2154	–	$\nu_a(^{12}C^{14}N)$
2136	–	$\nu_a(^{12}C^{15}N)$
2128	–	$\nu_a(^{12}C^{15}N)$
2122	–	$\nu_a(^{13}C^{14}N)$
2113	–	$\nu_a(^{13}C^{14}N)$
1684	–	δ(HOH) coordinated water
1636	–	δ(HOH) uncoordinated water
590	–	δ(CoCN)
563	–	δ(CoCN)
–	496	δ(CoCN)
–	481	ν_s(C—Co—C)
–	466	ν_s(C—Co—C)
455	–	ν_a(C—Co—C)
446	–	ν(Y—OH_2)
–	249	?
–	221	?
–	85	δ(CoCN) + δ(CCoC)

assigned to the ν(OH) stretching modes corresponding to uncoordinated water molecules (hydrogen-bonded bands). The bending mode of water molecules appears as a doublet in the IR spectrum at 1684 and 1636 cm^{-1} due to the presence of different types of water molecules [30–33]. The band located at higher wavenumber is attributed to water with a strong interaction with Y^{3+} (coordinated water) and the band at lower wavenumber corresponds to the weakly bonded water (uncoordinated or hydrogen-bonded water). This assignment is in agreement with the results reported by different authors who have studied the vibrational behavior of different hexacyanometallates [1,3,30–33].

The librational modes of coordinated water generally are difficult to identify because they show low intensity and are overlapped with other modes. The band located at 717 and 646 cm^{-1} are assigned to rocking and wagging vibrational modes, respectively. The band observed at 446 cm^{-1} could be attributed to Y—OH_2 stretching vibration [3].

3.3. Thermal decomposition

The thermal behavior of the $Y[Co(CN)_6]\cdot 4H_2O$ was studied by means TG and DT analysis. Fig. 5 shows TG and DTA curves from the thermal decomposition of the complex measured in flowing air. The first step ends at 170 °C with a mass loss of 14.80% and it corresponds to the loss of three water molecules. The second step ends at 230 °C with a mass loss of 4.57% and it is attributed to the loss of one water molecule. These two steps are accompanied by two endothermic peaks at 133 and 176 °C in the DTA curve. The third decomposition step occurs in the temperature range of 230–480 °C and it could be attributed to the elimination and oxidation of all the CN groups, but part of the CO_2 formed in this combustion clearly gets adsorbed on the surface of the particles as carbonate species, in this way, we cannot observe the mass loss corresponding to 6 CN groups. The exothermic peak located at 367 °C in the DTA curve is attributed to the decomposition step mentioned later. The mass loss observed at temperatures higher than 480 °C was assumed to be due to the decomposition of carbonate species derived from the oxidation

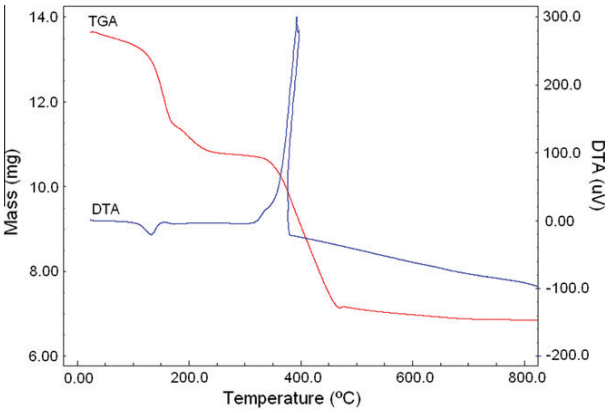

Fig. 5. TGA and DTA curves for $Y[Co(CN)_6]\cdot 4H_2O$ in air.

of CN groups. At temperatures higher than 800 °C the mass remains constant.

3.4. Thermal treatments of $Y[Co(CN)_6]\cdot 4H_2O$ at different temperatures

In order to know which is the lower temperature of synthesis of $YCoO_3$ perovskite-type oxide as a pure phase, thermal treatments of $Y[Co(CN)_6]\cdot 4H_2O$ in furnace at different temperatures were carried out. The qualitative composition of the residues at different temperatures was determined using X'Pert Highscore Program (version 2.1b). The PXRD patterns of the residues obtained by decomposition of $Y[Co(CN)_6]\cdot 4H_2O$ heated at different temperatures for 6 h are shown in Fig. 6a. When the complex was heated at 650 and 750 °C, the peaks attributed to Y_2O_3 and Co_3O_4 were observed. When we increased the calcination temperature to 850 °C, some peaks attributed to $YCoO_3$ were observed accompanied to some peaks assigned to Y_2O_3. When the complex was treated at 950 °C, all the peaks are attributable to orthorhombic $YCoO_3$ and small diffraction peaks assigned to Y_2O_3 were observed as an impurity. A similar result was observed for $YFeO_3$ prepared by thermal decomposition of $Y[Fe(CN)_6]\cdot 4H_2O$ [14]. This result demonstrated that the decomposition of cyano-complexes is better to prepare perovskite-type oxides at low temperature than ceramic methods [12–20]. The PXRD of $YCoO_3$ obtained at 950 °C was refined by means the Rietveld method as shown in Fig. 6b. Some evidence for unreacted Y_2O_3 was seen in the diffraction data, because of this, vacancies on the Y^{3+} site in $YCoO_3$ were also refined. Results of the complete structural refinement for $YCoO_3$ prepared at 950 °C are shown in Table 4. The oxide $YCoO_3$ crystallizes in a distorted perovskite structure with an orthorhombic unit cell. The distortion from the ideal perovskite is mainly in the position of the Y^{3+} ions, whereas the Co^{3+} ions are present in an essentially octahedral environment. $YCoO_3$ perovskite has an yttrium–defficient structure and we can write the formula as $Y_{0.961}CoO_3$.

Fig. 7a shows the FTIR spectrum of $YCoO_3$ prepared at 950 °C in air atmosphere. The bands located between 1700 and 1300 cm^{-1} could be attributed to carbonate species formed by CO_2 adsorption. Asamoto et al. have reported two types of carbonate species formed by thermal decomposition of cyano complexes; one is the bidentate-type carbonate produced by oxidation of CN groups and the other is the monodentate-type carbonate formed by CO_2 adsorption [34]. The bands located at 639 and 564 cm^{-1} could be assigned to the O—Co—O stretching vibration. The splitting of the intermediate bands could be attributed to a dynamic Jahn–Teller distortion of Co^{3+} ions in intermediate spin state [35].

The Raman spectrum of $YCoO_3$ measured at room temperature is shown in Fig. 7b. The Raman active modes of the *Pnma* struc-

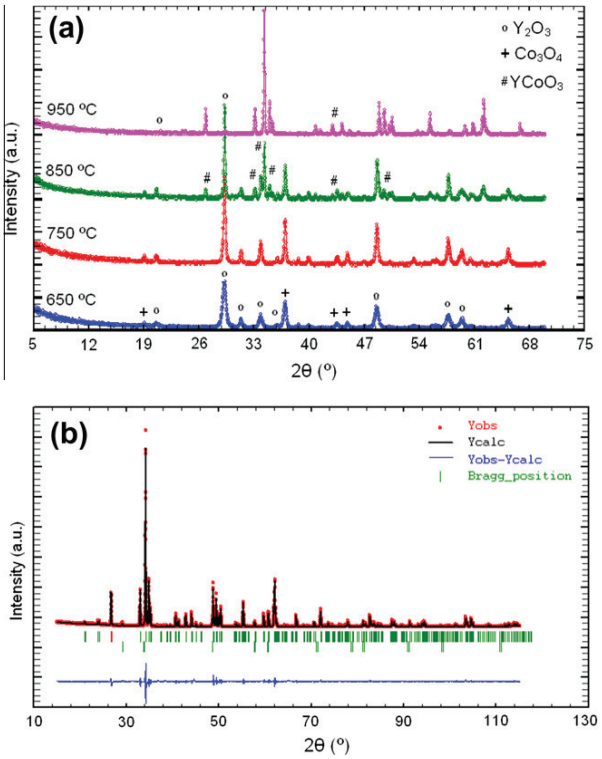

Fig. 6. (a) PXRD patterns of residues obtained by heat treatment of $Y[Co(CN)_6]\cdot 4H_2O$ at different temperatures. (b) Rietveld refinement of PXRD pattern for $YCoO_3$ obtained at 950 °C.

Table 4
Crystallographic parameters for $YCoO_3$ obtained by thermal decomposition of $Y[Co(CN)_6]\cdot 4H_2O$ at 950 °C, after Rietveld refinement with PXRD data.

Atom	Wyckoff site	*x*	*y*	*z*	Occupancy
Co	4b	0	0	0.5	1.0
Y	4c	0.06869(8)	0.25	0.9827(1)	0.961(1)
O1	4c	0.9731(5)	0.25	0.4044(6)	1.0
O2	8d	0.3013(4)	0.0507(3)	0.6929(4)	1.0

Space group: *Pnma*; cell parameters: $a = 5.4177(6)$ Å, $b = 7.3642(1)$ Å, $c = 5.1364(1)$ Å $V = 204.93(4)$, $Z = 4$
Wt. Fraction of $Y_2O_3 = 4.02\%$.

ture are 7 A_g + 7 B_{1g} + 5 B_{2g} + 5 B_{3g} and the non-zero components of the Raman tensors are (*xx*,*yy*,*zz*), (*xy*), (*xz*) and (*yz*) for A_g, B_{1g}, B_{2g} and B_{3g} representations, respectively [36]. The representation $A_g + B_{1g}$ belongs to symmetric modes and 2 B_{2g} and 2 B_{3g} belongs to antisymmetric stretching modes. Here $A_g + 2B_{2g} + B_{3g}$ and 2 $A_g + B_{1g} + 2$ $B_{2g} + B_{3g}$ are related to rotation and tilt modes of the octahedral CoC_6, and 3 $A_g + 3$ $B_{1g} + B_{2g} + B_{3g}$ is related to the rare earth movements. The main peaks of the *Pnma* structure of $YCoO_3$ correspond to the following modes and symmetries: the symmetric stretching of the CoO_6 octahedra is observed at 640 cm^{-1} (B_{1g} symmetry), the antisymmetric stretching is observed at around 564 cm^{-1} (A_g symmetry) associated with the Jahn–Teller distortion, and the tilt of the octahedral CoO_6 is observed at around 351 cm^{-1} (A_g symmetry) as a strong band [35]. The modes at low wavenumbers are those related to the Y^{3+} movements and lattice vibrations. It is clear that Raman spectroscopy has the advantage of sensivity to structure distortion and oxygen motions.

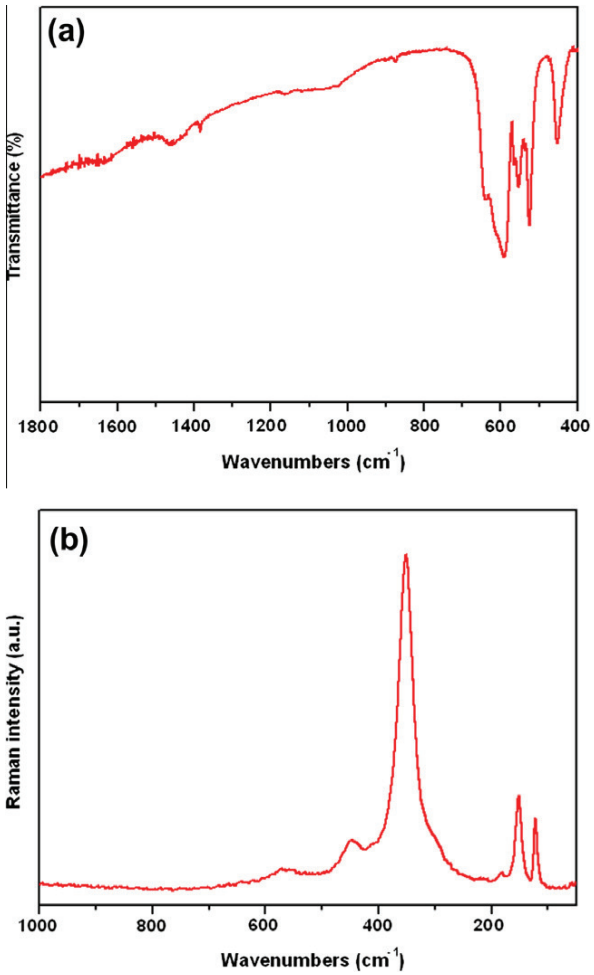

Fig. 7. (a) IR spectrum of $YCoO_3$ obtained at 950 °C between 1800 and 400 cm^{-1}. (b) Raman spectrum of $YCoO_3$.

4. Conclusions

The crystal structure of the cyano complex $Y[Co(CN)_6]\cdot 4H_2O$ was refined by means the Rietveld analysis. The complex crystallizes in the orthorhombic crystal system, space group Cmcm, cell parameters $a = 7.2947(1)$ Å, $b = 12.6654(2)$ Å, $c = 13.5224(2)$ Å. In this structure the Y^{3+} ions are eight coordinated to six nitrogen atoms from CN groups and two oxygens from crystal water in the form of YN_6O_2 group. On the other hand, six carbon atoms are coordinated to a cobalt atom in octahedral geometry. Two uncoordinated water molecules occupy zeolitic holes.

The vibrational spectra of the complex are well-resolved so that features due to the stretching modes involving isotopes of minor abundance are clearly observed in the IR spectrum. The Raman spectrum showed two distinct set of bands of ν(CN): one was a singlet and the other was split. This implies that the symmetry around Y^{3+} is lower than that of other complexes having five water molecules.

The thermal decomposition of $Y[Co(CN)_6]\cdot 4H_2O$ in air was studied using TGA/DTA analysis. It decomposes in four steps. The first one corresponds to the elimination of three water molecules and the second one to the elimination of remanent water. The third step is associated to the elimination and oxidation of all CN groups. The last step corresponds to the elimination of CO_2 adsorbed in the surface of the particles as carbonate.

The thermal treatments of $Y[Co(CN)_6]\cdot 4H_2O$ in air produce the mixed oxide $YCoO_3$. We refine the structure of the mixed oxide obtained at 950 °C and found that it was slightly deficient in Y, which is in agreement with the small amount of Y_2O_3 found as an impurity in the sample. The formula of the orthorhombic phase should be written as $Y_{0.961}CoO_3$.

Acknowledgements

R.E.C. thanks FONCYT for PICT2007 303, CONICET for PIP #11220090100995 and SECyT-UNC for the Project 162/12. D.M.G. thanks CONICET for a fellowship. D.M.G. and M.I.G. thank CIUNT for financial support, Project 26D-428.

References

[1] M. Avila, L. Reguera, J. Rodriguez-Hernandez, J. Balmaseda, E. Reguera, J. Solid State Chem. 181 (2008) 2899–2907.
[2] R. Martinez-Garcia, L. Reguera, M. Knobel, E. Reguera, J. Phys.: Condens. Matter. 19 (2007) 1–11.
[3] D.M. Gil, M.C. Navarro, M.C. Lagarrigue, J. Guimpel, R.E. Carbonio, M.I. Gómez, J. Mol. Struct. 1003 (2011) 129–133.
[4] J. Rodriguez-Hernandez, A. Gomez, E. Reguera, J. Phys. D: Appl. Phys. 40 (2007) 6076–6087.
[5] F. Hulliger, M. Landolt, H. Vestch, J. Solid State Chem. 18 (1976) 307–312.
[6] M.C. Navarro, E.V. Pannunzio-Miner, S. Pagola, M.I. Gómez, R.E. Carbonio, J. Solid State Chem. 178 (2005) 847–854.
[7] L. Wu, J. Yu, L. Zhang, X. Wang, S. Li, J. Solid State Chem. 177 (2004) 3666–3674.
[8] X. Lu, J. Xie, H. Shu, J. Liu, C. Yin, J. Lin, Mater. Sci. Eng. B. 138 (2007) 289–292.
[9] J. Lentmaier, S. Kemmler-Sack, G. Knell, P. Kessler, P. Plies, Mater. Res. Bull. 31 (1996) 1269–1276.
[10] J. Lentmaier, S. Kemmler-Sack, Mater. Res. Bull. 33 (1998) 461–473.
[11] J. Dho, W.S. Kim, E.O. Chi, N.H. Hur, S.H. Park, H.C. Ri, Solid State Commun. 125 (2003) 143–147.
[12] P.K. Gallagher, Mater. Res. Bull. 3 (1968) 225–232.
[13] E. Traversa, P. Nunziante, M. Sakamoto, Y. Sadaoka, M.C. Carotta, G. Martinelli, J. Mater. Res. 13 (1998) 1335–1345.
[14] D.M. Gil, M.C. Navarro, M.C. Lagarrigue, J. Guimpel, R.E. Carbonio, M.I. Gómez, J. Therm. Anal. Calorim. 103 (3) (2011) 889–896.
[15] D.M. Gil, R.E. Carbonio, M.I. Gómez, J. Chil. Chem. Soc. 55 (2010) 189–192.
[16] M.C. Navarro, M.C. Lagarrigue, J.M. De Paoli, R.E. Carbonio, M.I. Gómez, J. Therm. Anal. Calorim. 102 (2010) 655–660.
[17] L. Medina Córdoba, M.I. Gómez, J.A. Morán, P.J. Aymonino, J. Argent. Chem. Soc. 96 (1–2) (2008) 1–12.
[18] L. Medina Córdoba, J.A. Morán, S. Santos Jr, O.E. Piro, M.I. Gómez, J. Chem. Crystallogr. 41 (9) (2011) 1280–1284.
[19] D.M. Gil, M. Avila, E. Reguera, S. Pagola, M.I. Gomez, R.E. Carbonio, Polyhedron 33 (2012) 450–455.
[20] Y. Itagaki, M. Mori, Y. Hosoya, H. Aono, Y. Sadaoka, Sensor Actuators B 122 (2007) 315–320.
[21] R.A. Young, The Rietveld Method, Oxford Scientifics Publications, UK, 1995.
[22] J. Rodriguez-Carbajal, Physica B 192 (1993) 55–69.
[23] A. Dommann, H. Vetsch, F. Hulliguer, Acta Cryst. C 46 (1990) 1992–1994.
[24] L.W. Finger, D.E. Cox, A.P. Jephcoat, J. Appl. Cryst. 27 (1994) 892–900.
[25] D.F. Mullica, P.K. Hayward, E.L. Sappenfield, Acta Cryst. C 52 (1996) 61–63.
[26] D.F. Mullica, D.L. Sappenfield, J. Solid State Chem. 82 (1989) 168–171.
[27] T. Pretsch, K.W. Chapman, G.J. Halder, C.J. Kepert, Chem. Commun. (2006) 1857–1859.
[28] K. Nakamoto, Infrared and Raman Spectra of Inorganic and Coordination Compounds, Wiley, New York, 1986.
[29] Y. Yukawa, S. Igarashi, T. Kawaura, H. Miyamoto, Inorg. Chem. 35 (1996) 7399–7403.
[30] L.P. Zhang, X. Zhou, T.C.W. Mak, P.A. Tanner, Polyhedron 26 (2007) 4019.
[31] W. Xiaoyu, Y. Yukawa, Y. Masuda, J. Alloys Compd. 290 (1999) 85.
[32] A. Gómez, E. Reguera, Int. J. Inorg. Mater. 3 (2001) 1045.
[33] M. Avila, L. Reguera, C. Vargas, E. Reguera, J. Phys. Chem. Solids 70 (2009) 477.
[34] M. Asamoto, H. Yahiro, Catal. Surv. Asia 13 (2009) 221–228.
[35] I.G. Main, J.F. Marshall, G. Demazeau, G.A. Robins, C.E. Johnson, J. Phys. C: Solid State Phys. 12 (1979) 2215–2224.
[36] F.A. Cotton, Teoría de grupos aplicada a la química, Limusa, México, 1977.